EUROPEAN ORGANIZATION FOR NUCLEAR RESEARCH

$_\Lambda^3$H and $_\Lambda^3\overline{\text{H}}$ production in Pb–Pb collisions at $\sqrt{s_{\text{NN}}}$ = 2.76 TeV

ALICE Collaboration[*]

Abstract

The production of the hypertriton nuclei $_\Lambda^3$H and $_\Lambda^3\overline{\text{H}}$ has been measured for the first time in Pb–Pb collisions at $\sqrt{s_{\text{NN}}}$ = 2.76 TeV with the ALICE experiment at LHC energies. The total yield, $\text{d}N/\text{d}y \times \text{B.R.}_{\left(_\Lambda^3\text{H}\to^3\text{He},\pi^-\right)} = (3.86 \pm 0.77(\text{stat.}) \pm 0.68(\text{syst.})) \times 10^{-5}$ in the 0–10% most central collisions, is consistent with the predictions from a statistical thermal model using the same temperature as for the light hadrons. The coalescence parameter B_3 shows a dependence on the transverse momentum, similar to the B_2 of deuterons and the B_3 of ^{3}He nuclei. The ratio of yields $S_3 = {_\Lambda^3}\text{H}/(^3\text{He}\times\Lambda/\text{p})$ was measured to be $S_3 = 0.60 \pm 0.13$ (stat.) ± 0.21 (syst.) in 0–10% centrality events; this value is compared to different theoretical models. The measured S_3 is fully compatible with thermal model predictions. The measured $_\Lambda^3$H lifetime, $\tau = 181^{+54}_{-39}(\text{stat.}) \pm 33(\text{syst.})$ ps is compatible within 1σ with the world average value.

[*]See Appendix A for the list of collaboration members

arXiv:1506.08453v1 [nucl-ex] 28 Jun 2015

1 Introduction and Physics Motivations

High-energy heavy-ion collisions offer a unique way to study the behaviour of nuclear matter under conditions of extreme energy densities. At LHC energies, particles carrying strangeness are abundantly produced and light clusters of nucleons and hyperons, called hypernuclei, are expected to be formed [1]. Since their first observation [2], there has been a constant interest in searching for new hypernuclei as they offer an experimental way to study the hyperon-baryon (YN) and the hyperon-hyperon (YY) interactions, which are relevant for nuclear physics and nuclear astrophysics. For instance, the YN interaction plays a key role in understanding the structure of neutron stars [3–6]. The production of hypernuclei in heavy-ion collisions has been proposed and studied for a long time [7, 8] and at ultrarelativistic energies it is possible to produce particles otherwise inaccessible, such as anti-hypernuclei. In fact, while many Λ-hypernuclei have been observed, the first observation of an anti-hypernucleus is rather recent and was reported from the analysis of Au–Au collisions at $\sqrt{s_{\text{NN}}} = 200$ GeV by the STAR Collaboration at RHIC [9]. Since hypernuclei are weakly bound nuclear systems, they are sensitive probes of the final stages of the evolution of the fireball formed in the heavy-ion collisions [10]. The yield of hypernuclei can distinguish between different production scenarios, usually described using two different theoretical approaches. The first one is based on a coalescence model [11], while the second one is based on the assumption that all the particle species can be described using a statistical thermal model [12]. In the statistical thermal model a constant entropy over baryon ratio [13] could explain why objects with such a small binding energy (few MeV) could survive the high temperature (≈ 170 MeV) expanding fireball. On the other hand, if hypernuclei are produced through coalescence of protons, neutrons and hyperons at freeze-out [14], they will provide a measurement of the local correlation between baryons and hyperons (strangeness) [15].

This letter presents a study of hypertriton and anti-hypertriton production at $\sqrt{s_{\text{NN}}} = 2.76$ TeV Pb–Pb collisions by the ALICE collaboration. The paper is organised as follows. In Section 2 the ALICE detector is briefly described. The data sample, analysis details and systematic uncertainties are presented in Section 3. In Section 4 the obtained results are compared with theoretical models. Finally the conclusions are drawn in Section 5.

2 The ALICE detector

A detailed description of the ALICE detector can be found in [16] and references therein. For the present analysis the main sub-detectors used are the V0 detectors, the Inner Tracking System (ITS) and the Time Projection Chamber (TPC), which are located inside a 0.5 T solenoidal magnetic field. The V0 [17] detectors are placed around the beam-pipe on either side of the interaction point: one covering the pseudorapidity range $2.8 < \eta < 5.1$ (V0-A) and the other one covering $-3.7 < \eta < -1.7$ (V0-C). The collision centrality is estimated by using the multiplicity measured in the V0 detectors along with a Glauber model simulation to describe the multiplicity distribution as a function of the impact parameter [18, 19]. The ITS [20] has six cylindrical layers of silicon detectors with radii between 3.9 and 43 cm from the beam axis, covering the full azimuthal angle and the pseudorapidity range of $|\eta| < 0.9$. The same pseudorapidity range is covered by the TPC [21], which is the main tracking detector. Hits in the ITS and found clusters in the TPC are used to reconstruct charged-particle tracks. These are used to determine the primary collision vertex with a resolution of about 10 μm in the direction transverse to the beams for heavy-ion collisions. The TPC is used for particle identification through the dE/dx (specific energy loss) in the TPC gas.

3 Analysis

The (anti-)hypertriton (${}^{3}_{\Lambda}\overline{\text{H}}$) ${}^{3}_{\Lambda}$H is the lightest observed hypernucleus and is a bound state formed by a (anti-)proton, a (anti-)neutron and a (anti-)Λ. The ${}^{3}_{\Lambda}$H and ${}^{3}_{\Lambda}\overline{\text{H}}$ production yields were measured by

detecting their mesonic decay (${}^{3}_{\Lambda}\text{H} \rightarrow {}^{3}\text{He} + \pi^{-}$) and (${}^{3}_{\Lambda}\overline{\text{H}} \rightarrow {}^{3}\overline{\text{He}} + \pi^{+}$) via the topological identification of secondary vertices and the analysis of the invariant mass distributions of (${}^{3}\text{He}+\pi^{-}$) and (${}^{3}\overline{\text{He}}+ \pi^{+}$) pairs.

The analysis was done using Pb–Pb collisions at $\sqrt{s_{\text{NN}}} = 2.76$ TeV taken in 2011. The events were collected with an interaction trigger requiring a signal in both V0-A and V0-C. Only events with a primary vertex reconstructed within ± 10 cm, along the beam axis, from the nominal position of the interaction point were selected. The analysed sample, collected with two different centrality trigger configurations corresponding to the 0–10% and 10–50% centrality intervals, contained approximately 20×10^{6} and 17×10^{6} events, respectively.

The ${}^{3}_{\Lambda}\text{H}$ can be identified via the invariant mass of its decay products and, since it has a lifetime similar to the free Λ ($c\tau \sim 8$ cm), in most cases it is possible to identify its decay up to a few cm away from the primary vertex. The decay vertex was determined by exploiting a set of geometrical selections: i) the Distance of Closest Approach (DCA) between the two particle tracks identified using dE/dx in the TPC as ${}^{3}\text{He}$ and π, ii) the DCA of the $\pi^{\pm}$ tracks from the primary vertex, iii) the cosine of the angle between the total momentum of the decay pairs at the secondary vertex and a vector connecting the primary vertex and the secondary vertex (pointing angle), and iv) a selection on the proper lifetime ($c\tau$) of the candidate. An additional selection on the ${}^{3}_{\Lambda}\text{H}$ (${}^{3}_{\Lambda}\overline{\text{H}}$) rapidity ($|y| < 0.5$) was applied.

Figure 1 shows the invariant mass distribution of (${}^{3}\text{He},\pi^{-}$) on the left and (${}^{3}\overline{\text{He}},\pi^{+}$) on the right for events with 10–50% centrality in the pair transverse momentum range $2 \leq p_{\text{T}} < 10$ GeV/c. In order to estimate the background, for each event the π track detected at the secondary vertex was rotated 20 times by a random azimuthal angle. The shape of the corresponding (${}^{3}\text{He}, \pi$) invariant mass distribution was found to reproduce the observed background outside the signal region. The data points were fitted with a function which is the sum of a Gaussian and a third degree polynomial, used to describe the signal and the background, respectively. The background was normalized to the measured values in the $3.01 - 3.08$ GeV/c^2 region. The fit to the background distribution was used to fix the parameters of the polynomial in the combined fit.
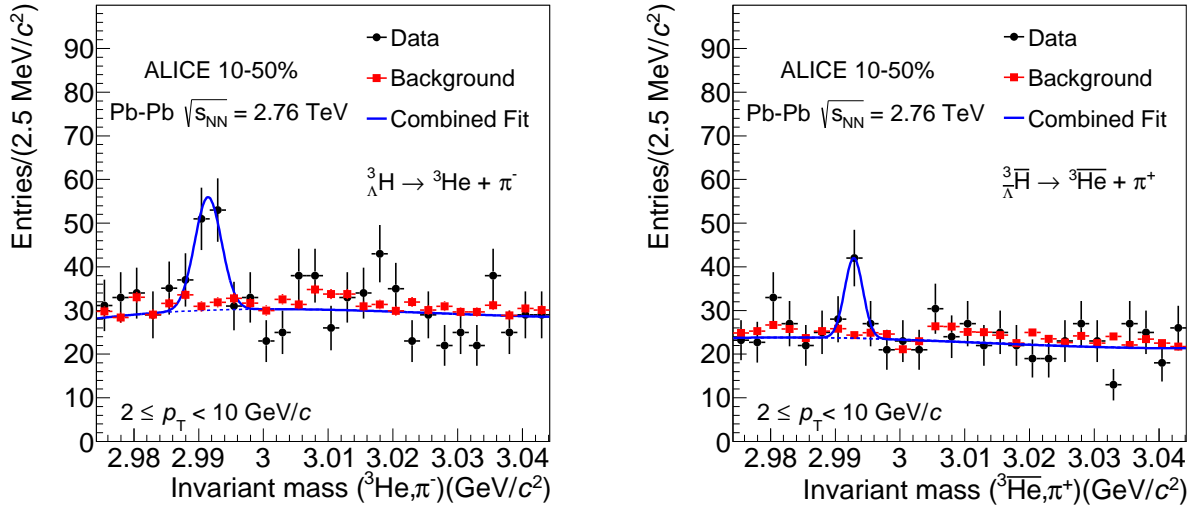

Figure 1: Invariant mass of (${}^{3}\text{He},\pi^{-}$) (left) and (${}^{3}\overline{\text{He}},\pi^{+}$) (right) for events with 10–50% centrality in the pair $2 \leq p_{\text{T}} < 10$ GeV/c interval. The data points are shown as full circle, while the squares represent the background distribution as described in the text. The curve represents the function used to perform the fit and used to evaluate the background and the raw signal.

In the 0–10% most central collisions, a signal was extracted in three transverse momentum intervals ($2 \leq p_{\text{T}} < 4$ GeV/c, $4 \leq p_{\text{T}} < 6$ GeV/c, $6 \leq p_{\text{T}} < 10$ GeV/c) , for both ${}^{3}_{\Lambda}\text{H}$ and ${}^{3}_{\Lambda}\overline{\text{H}}$. In the 10–50% cen-

trality class a signal both for ${}^3_\Lambda$H and ${}^3_\Lambda\overline{\text{H}}$ was obtained for the full p_T range under study ($2 \leq p_\text{T} < 10\,\text{GeV}/c$). From the combined fit results the mean value, the width and the yield of the signal were extracted. The mean invariant mass ($\mu = 2.991 \pm 0.001$ (stat.) $\pm\,0.003$ (syst.) GeV/c^2) is compatible within uncertainties with the mass from the literature [22]. The signal width, $\sigma = (3.01 \pm 0.24\,\text{(stat.)}) \times 10^{-3}\text{GeV}/c^2$ obtained as the mean value of all the measured widths, is reproduced by Monte Carlo simulations and is driven by detector resolution. The raw yield of the signal was defined as the integral of the Gaussian function in a $\pm\,3\,\sigma$ region around the mean value.

A correction factor which takes into account the detector acceptance, the reconstruction efficiency, and the absorption of ${}^3_\Lambda$H (${}^3_\Lambda\overline{\text{H}}$) by the material crossed was determined as a function of p_T. Detector acceptance and reconstruction efficiency were evaluated using a dedicated HIJING Monte Carlo simulation [23], where the only allowed decay was the two-body decay to charged particles, (${}^3_\Lambda\text{H} \to {}^3\text{He} + \pi^-$) and (${}^3_\Lambda\overline{\text{H}} \to {}^3\overline{\text{He}} + \pi^+$). The simulated particles were propagated through the detector using the GEANT3 transport code [24] and then processed with the same reconstruction chain as for the data.

Since the absorption of (anti-)(hyper)nuclei is not properly implemented in GEANT3, a correction based on the p ($\overline{\text{p}}$) absorption was applied in order to take into account the absorption of ${}^3_\Lambda$H (${}^3_\Lambda\overline{\text{H}}$) and ${}^3\text{He}$ (${}^3\overline{\text{He}}$) by the material of the ALICE detector. In this approach, the ${}^3\text{He}$ and ${}^3_\Lambda$H were treated as states of three independent p ($\overline{\text{p}}$). To take into account the small Λ separation energy ($B_\Lambda({}^3_\Lambda\text{H}) = 0.13 \pm 0.05$ MeV [25]), the absorption cross section of the ${}^3_\Lambda$H was increased by 50% with respect to the one of the ${}^3\text{He}$, as an intermediate value chosen between the absorption correction of ${}^3\text{He}$ and twice its value. The correction applied to the extracted yield was about 12% for ${}^3_\Lambda$H and about 22% for ${}^3_\Lambda\overline{\text{H}}$. The total systematic uncertainty takes into account, as lower and upper limits of the ${}^3_\Lambda$H(${}^3_\Lambda\overline{\text{H}}$) absorption cross section, values respectively equal to or two times higher than the absorption cross section of ${}^3\text{He}$(${}^3\overline{\text{He}}$). This uncertainty is p_T dependent, and its values are reported in Table 1. Other sources of systematic uncertainties in the yield evaluation were estimated:

- The systematic uncertainty due to the single-track efficiency, and the different choices of the track quality selections was taken from [26]. A 10% uncertainty is quoted for the two body decay of ${}^3_\Lambda$H.

- ${}^3_\Lambda$H lifetime: since the ${}^3_\Lambda$H lifetime is not accurately known, the influence of varying the ${}^3_\Lambda$H lifetime on the efficiency was evaluated by variation of the proper lifetime of the injected ${}^3_\Lambda$H in the Monte Carlo simulation. The associated uncertainty was estimated using two additional dedicated Monte Carlo simulations with different lifetimes. The injected lifetime of ${}^3_\Lambda$H (${}^3_\Lambda\overline{\text{H}}$) was varied ($\pm 1\sigma$) with respect to the result obtained in this analysis, leading to an uncertainty of 8.5%.

- The uncertainty related to the signal extraction procedure was evaluated by constraining fit parameters (μ and σ) in different ways. This source led to a 9% uncertainty.

The systematic uncertainty due to the uncertainty of the ALICE detector material budget and p_T distribution in the Monte Carlo used for the efficiency estimation led to a 1% systematic uncertainty.

The ${}^3_\Lambda$H and ${}^3_\Lambda\overline{\text{H}}$ spectra are shown in Figure 2 (left panel), multiplied by the branching ratio (B.R.) of the ${}^3_\Lambda\text{H} \to {}^3\text{He} + \pi^-$ decay. The anti-hypertriton to hypertriton ratio as a function of p_T is shown in Figure 2 (right panel). It is consistent with unity over the whole considered p_T range, as expected from zero net baryon density at LHC energies. In the ratio, the common systematic uncertainties (tracking efficiency, lifetime, and signal extraction method) cancel out and have therefore been removed.

In order to take into account the unmeasured p_T region and to extract the particle yields integrated over the full p_T range, the spectra were fitted using a blast-wave function [27] whose parameter values were taken from the combined deuteron and ${}^3\text{He}$ analysis [28] leaving the normalization free . The extrapolation in the $p_\text{T} < 2\,\text{GeV}/c$ region contributes 28% to the final yield for both ${}^3_\Lambda$H and ${}^3_\Lambda\overline{\text{H}}$, while the
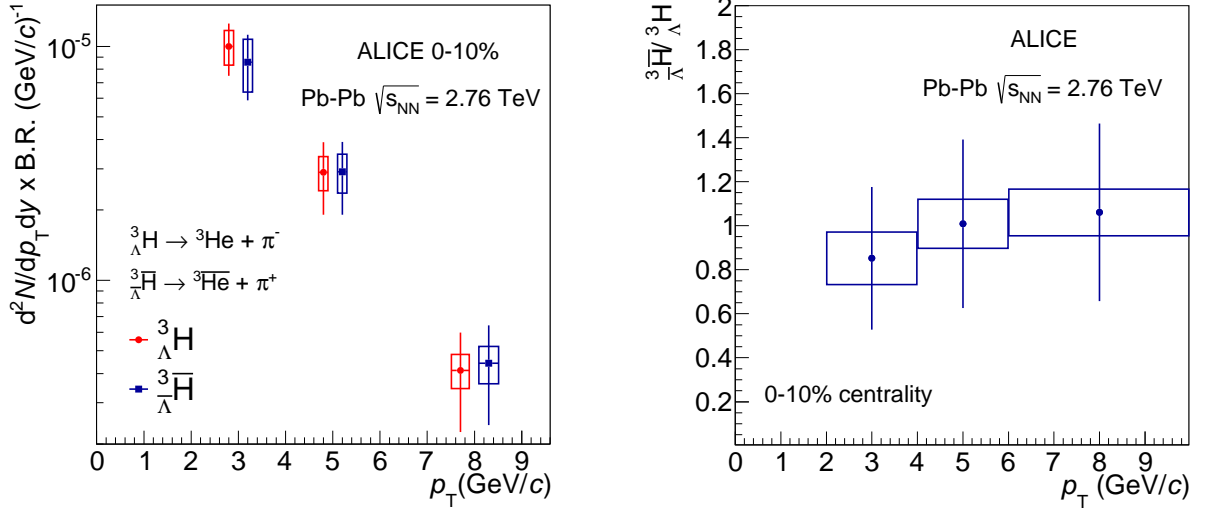
Figure 2: Left: Transverse momentum spectra multiplied by the B.R. of the ${}^{3}_{\Lambda}$H $\rightarrow {}^{3}$He $+ \pi^{-}$ decay for ${}^{3}_{\Lambda}$H (full circle) and ${}^{3}_{\Lambda}\overline{\text{H}}$ (squares) for the most central (0–10%) Pb–Pb collisions at $\sqrt{s_{NN}} = 2.76$ TeV for $|y| < 0.5$. Symbols are displaced for better visibility. Right: ${}^{3}_{\Lambda}\overline{\text{H}}$ to ${}^{3}_{\Lambda}$H ratio as a function of p_{T}. In both panels statistical uncertainties are represented by bars and systematic uncertainties are represented by open boxes.

contribution for $p_{T} > 10$ GeV/c is negligible. Different transverse momentum distributions were used to evaluate the systematic uncertainty related to the extrapolation, which was found to be 5%.

	${}^{3}_{\Lambda}$H				${}^{3}_{\Lambda}\overline{\text{H}}$			
	p_{T} intervals (GeV/c)				p_{T} intervals (GeV/c)			
	2–4	4–6	6–10	2–10	2–4	4–6	6–10	2–10
Absorption	5.4%	5.3 %	5.4%	5.4%	13%	10%	8.9 %	10.6%
Tracking efficiency	10 %	10 %	10 %	10 %	10 %	10 %	10 %	10 %
${}^{3}_{\Lambda}$H lifetime	8.5%	8.5%	8.5%	8.5 %	8.5%	8.5%	8.5%	8.5 %
Signal extraction method	9 %	9 %	9 %	9 %	9 %	9 %	9 %	9 %
Extrapolation at low p_{T}	5 %	5 %	5 %	5 %	5 %	5 %	5 %	5 %
Total	17.5%	17.5%	17.5%	17.5%	21.1%	19.4%	18.9%	19.8 %

Table 1: Summary of systematic uncertainties for the three p_{T} intervals and in the full range considered. These uncertainties are the same for events with 0–10% and 10–50% centrality. For the final systematic uncertainty evaluation they were added in quadrature.

To determine the lifetime, the (${}^{3}_{\Lambda}$H $+$ ${}^{3}_{\Lambda}\overline{\text{H}}$) sample was divided into four intervals in $ct = MLc/p$, where M is the mass, L the decay length, c is the speed of light, and p is the total momentum. The mass was fixed to the value from the literature $M = 2.991$ GeV/c^{2} [22]. For the determination of the lifetime, both centrality classes 0–10% and 10–50% were used. The signal was extracted in the intervals: $1 \leq ct < 4$ cm, $4 \leq ct < 7$ cm, $7 \leq ct < 10$ cm and $10 \leq ct < 28$ cm. To estimate the lifetime, the raw signal was corrected by the detector acceptance, the reconstruction efficiency and the absorption of ${}^{3}_{\Lambda}$H (${}^{3}_{\Lambda}\overline{\text{H}}$) in the material. The same dedicated HIJING Monte Carlo simulation and the same procedure used to determine the p_{T} dependence of the efficiency were used. The sources of systematic uncertainty are shown in Table 2.

An exponential fit was performed to determine the lifetime. The dN/d(ct) distribution and the exponential fit are shown in Figure 3. The vertical bars show the statistical uncertainties and the boxes represent the

Source	Value
Signal extraction method	9%
Tracking Efficiency	10%
Absorption	12%
Total	18%

Table 2: Summary of systematic uncertainties for the determination of the proper lifetime of $^{3}_{\Lambda}$H+$^{3}_{\Lambda}\overline{\text{H}}$.

systematic uncertainties.

The slope of the fit results in a proper decay length of $c\tau = \left(5.4^{+1.6}_{-1.2}(\text{stat.}) \pm 1.0(\text{syst.})\right)$ cm. To determine the statistical error the Minuit processor `MINOS` embedded in the ROOT framework [29] was used.
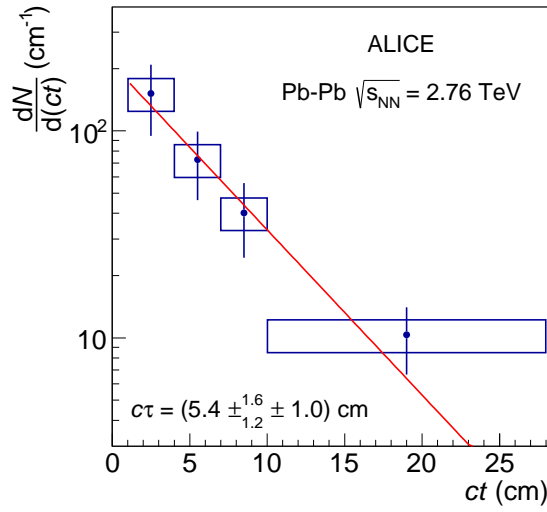

Figure 3: Measured dN/d(ct) distribution and an exponential fit used to determine the lifetime. The bars and boxes are the statistical and systematic uncertainties, respectively.

The lifetimes of light Λ-hypernuclei ($A \leq 4$) are expected to be very similar to that of the free Λ, if the Λ in the hypernucleus is weakly bound [31]. The measured lifetimes of light hypernuclei such as $^{3}_{\Lambda}$H [9, 32–38] are not known as precisely as the Λ lifetime, and theoretical predictions [31,39–46] are scattered over a large range, too. Recently, a statistical combination of the experimental lifetime estimations of $^{3}_{\Lambda}$H available in literature was published, resulting in an average value $\tau = \left(216^{+19}_{-18}\right)$ ps [47].

With the present data, a lifetime of $\tau = \left(181^{+54}_{-39}(\text{stat.}) \pm 33(\text{syst.})\right)$ ps has been obtained. It is compared with the previously published results in Figure 4. Our result, together with the previous ones, was used to re-evaluate the world average of the existing results using the same procedure as described in [47]. The obtained value, $\tau = \left(215^{+18}_{-16} \text{ ps}\right)$, is shown as a band in Figure 4. The result obtained in this analysis is compatible with the computed average.

4   Comparison between experimental yields and theoretical models

The product of the total integrated yields and the B.R. of the $^{3}_{\Lambda}$H $\rightarrow$ (^{3}He + π^{-}) decay for $^{3}_{\Lambda}$H and $^{3}_{\Lambda}\overline{\text{H}}$ for two centrality classes (0–10% and 10–50%) are reported in Table 3. The systematic uncertainties also include the contribution due to the low p_{T} extrapolation as described in Section 3.

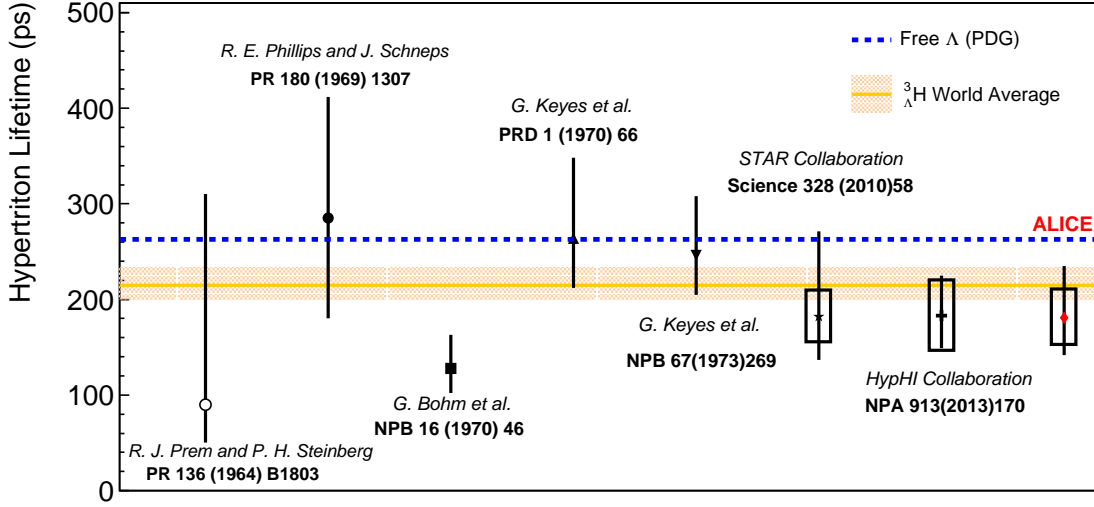It is possible to compare the production yields at different centralities by scaling them according to the

Figure 4: ${}^{3}_{\Lambda}$H lifetime (τ) measured by in this analysis (red diamond) compared with published results. The band represents the world average of ${}^{3}_{\Lambda}$H lifetime measurements $\left(\tau = 215^{+18}_{-16}\right)$ ps, while the dashed line represent the lifetime of Λ as reported by the Particle Data Group [30].

charged-particle densities $\langle \mathrm{d}N_{ch}/\mathrm{d}\eta \rangle$. For central (0–10%) collisions $\langle \mathrm{d}N_{ch}/\mathrm{d}\eta \rangle = 1447 \pm 39$, while for semi-central (10–50%) $\langle \mathrm{d}N_{ch}/\mathrm{d}\eta \rangle = 575 \pm 12$. The ratio

$$\frac{\left(\dfrac{\left({}^{3}_{\Lambda}\text{H} + {}^{3}_{\Lambda}\overline{\text{H}} \right)_{(0-10\%)}}{\left({}^{3}_{\Lambda}\text{H} + {}^{3}_{\Lambda}\overline{\text{H}} \right)_{(10-50\%)}} \right)}{\left(\dfrac{\langle \mathrm{d}N_{ch}/\mathrm{d}\eta \rangle_{(0-10\%)}}{\langle \mathrm{d}N_{ch}/\mathrm{d}\eta \rangle_{(10-50\%)}} \right)} = 1.34 \pm 0.35(\text{stat.}) \pm 0.24(\text{syst.}) \tag{1}$$

is compatible with unity within $1\,\sigma$. The ${}^{3}_{\Lambda}$H (${}^{3}_{\Lambda}\overline{\text{H}}$) production scales with centrality like the charged-particle production.

Centrality	$\langle \mathrm{d}N_{ch}/\mathrm{d}\eta \rangle$	${}^{3}_{\Lambda}\text{H} \times \text{B.R.} \times 10^{-5}$	${}^{3}_{\Lambda}\overline{\text{H}} \times \text{B.R.} \times 10^{-5}$
0–10%	1447 ± 39	$3.86 \pm 0.77(\text{stat.}) \pm 0.68(\text{syst.})$	$3.47 \pm 0.81(\text{stat.}) \pm 0.69(\text{syst.})$
10–50%	575 ± 12	$1.31 \pm 0.37(\text{stat.}) \pm 0.23(\text{syst.})$	$0.85 \pm 0.29(\text{stat.}) \pm 0.17(\text{syst.})$

Table 3: Total integrated yields times the B.R. of the ${}^{3}_{\Lambda}\text{H} \rightarrow ({}^{3}\text{He} + \pi^{-})$ decay, for ${}^{3}_{\Lambda}$H and ${}^{3}_{\Lambda}\overline{\text{H}}$ in Pb–Pb collisions at $\sqrt{s_{\text{NN}}} = 2.76$ TeV for different centrality classes in $|y| < 0.5$. For each centrality interval the average $\langle \mathrm{d}N_{ch}/\mathrm{d}\eta \rangle$ is also reported [18].

4.1 Comparison between thermal models and experimental yields

Since the decay branching ratio of the ${}^{3}_{\Lambda}\text{H} \rightarrow {}^{3}\text{He} + \pi^{-}$ was estimated only relative to the charged-pion channels [37], the corresponding value (B.R.=35%) provides an upper limit for the absolute branching ratio. On the other hand, a theoretical estimation for the ${}^{3}_{\Lambda}\text{H} \rightarrow {}^{3}\text{He} + \pi^{-}$ decay branching ratio, which also takes into account decays with neutral mesons decays, gave a B.R.=25% [31]. Assuming a possible variation on the B.R. in the range 15–35%, we show in Figure 5 a comparison of our result with different theoretical model calculations [1, 48, 49]. The measured $\mathrm{d}N/\mathrm{d}y \times$ B.R. is shown as a

horizontal line, where the band represent statistical and systematic uncertainties added in quadrature while the different theoretical models are shown as lines. The data are compared with the following models: two versions of the statistical hadronization model [1, 48] and the hybrid UrQMD model [49], which combines the hadronic transport approach with an initial hydrodynamical stage for the hot and dense phase of a heavy-ion collision. The two versions of the statistical hadronization model used are the equilibrium statistical model (GSI-Heidelberg), described in [1] and references therein, with a temperature T_{ch} = 156 MeV and the non-equilibrium thermal model (SHARE), described in [48] and references therein, with T_{ch} = 138.3 MeV, γ_q = 1.63 and γ_s = 2.08, where γ_q and γ_s represent the quark and strangeness phase space occupancy of the system created after the collision, respectively.

The non-equilibrium thermal model (SHARE) [48] overestimates the (anti-)hypertriton yield by a factor from 2 to 5 depending on the branching ratio (B.R.). For the branching ratio expected following [31] (B.R. = 25%) the equilibrium thermal model [1] (GSI-Heidelberg) and the hybrid UrQMD model [49] describe the data best.
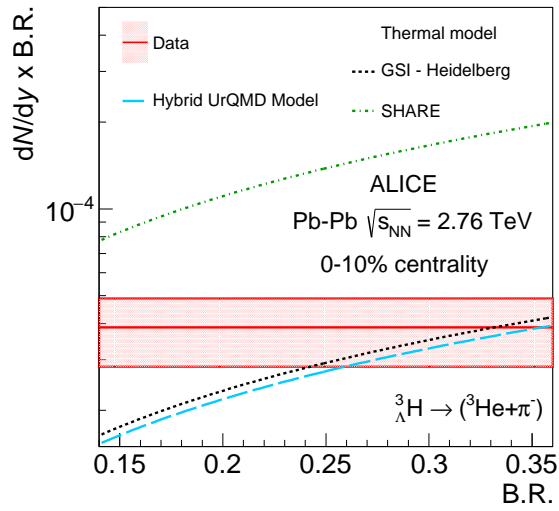

Figure 5: Yield times branching ratios as a function of branching ratio (dN/dy ×B.R. vs $B.R$). The horizontal line is the measured value and the band represents statistical and systematic uncertainties added in quadrature. Lines are different theoretical expectations as explained in the text.

A fit, based on the thermal fit described in [1], was performed to the hypertriton yield and to yields from other light flavour hadrons, except K*, previously measured by our Collaboration at $\sqrt{s_{\text{NN}}}$ = 2.76 TeV [28, 50–53]. The inclusion of the deuteron, ^{3}He [28] and ${}^{3}_{\Lambda}$H in the thermal fit [54] in addition to lighter particles, does not change the resulting freeze-out temperature (T_{ch} = 156 ± 2 MeV) and the measured yields of the nuclei and the hypertriton agree with the model predictions within 1 σ. The results on the hypertriton yields discussed above were also used to determine the ${}^{3}_{\Lambda}$H/^{3}He and ${}^{3}_{\Lambda}\overline{\text{H}}$/${}^{3}\overline{\text{He}}$ ratios, which are shown in Table. 4. In order to compute the ratios, our previous measurement of ^{3}He and ${}^{3}\overline{\text{He}}$ yields [28] were used.

These results were compared with different theoretical models [48, 55, 56] and results from the STAR experiment [9] at $\sqrt{s_{\text{NN}}}$ = 200 GeV, which use the same B.R. = 25%. The comparison is shown in Figure 6. STAR results are higher than ALICE results, but still compatible within uncertainties.

Centrality	${}^3_\Lambda$H / ^{3}He	${}^3_{\overline{\Lambda}}\overline{\text{H}}$ / ${}^3\overline{\text{He}}$
0–10%	$0.47 \pm 0.10(\text{stat.}) \pm 0.13(\text{syst.})$	$0.42 \pm 0.10(\text{stat.}) \pm 0.13(\text{syst.})$
10–50%	$0.40 \pm 0.11(\text{stat.}) \pm 0.11(\text{syst.})$	$0.26 \pm 0.09(\text{stat.}) \pm 0.08(\text{syst.})$

Table 4: Ratios of ${}^3_\Lambda$H/^{3}He and ${}^3_{\overline{\Lambda}}\overline{\text{H}}$/${}^3\overline{\text{He}}$ assuming a B.R. = 25% for the ${}^3_\Lambda$H $\to {}^3$He $+ \pi$ decay [31]. The results from ^{3}He and ${}^3\overline{\text{He}}$ analysis measured by the ALICE experiment were used [28].

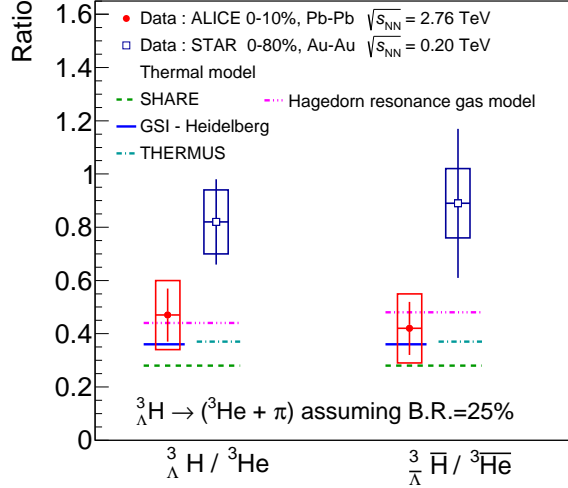**Figure 6:** The ratios ${}^3_\Lambda$H/^{3}He and ${}^3_{\overline{\Lambda}}\overline{\text{H}}$/${}^3\overline{\text{He}}$ determined by the present analysis (full circles) for matter and antimatter compared with STAR results (squares) [9] and theoretical predictions (lines) [1, 48, 55, 56] as described in the legend.

4.2 Data comparison to coalescence models and S_3 ratio

At the moment no prediction of the ${}^3_\Lambda$H and ${}^3_{\overline{\Lambda}}\overline{\text{H}}$ yields in a non-trivial dynamical coalescence model is available at LHC energies. Nevertheless within a simple coalescence model it is possible to evaluate some parameters which are sensitive to the existence of coalescence mechanisms for hypernuclei formation. In the empirical coalescence model [11] the cross section for the production of a cluster with mass number A is related to the probability that A nucleons have relative momenta less than p_0, which is a free parameter of the model. This provides the following relation between the production cross sections of the nuclear cluster emitted with a momentum p_A and the nucleon emitted with a momentum p_{p}

$$E_A \frac{\text{d}^3 N_A}{\text{d}^3 p_A} = B_A \left(E_{\text{p}} \frac{\text{d}^3 N_{\text{p}}}{\text{d}^3 p_{\text{p}}} \right)^A, \tag{2}$$

where $p_A = A p_{\text{p}}$. For a given nucleus, the coalescence parameter B_A should not depend on the momentum since it depends only on the cluster parameters:

$$B_A = \left(\frac{4\pi}{3} p_0^3 \right)^{(A-1)} \frac{M}{m^A} \tag{3}$$

where M and m are the nucleus and the proton mass, respectively. The parameter B_3 was computed for ${}^3_\Lambda$H according to Equation 2 using the spectrum shown in Figure 2 and our previous measurement of the

proton [50] and Λ [52] spectra.

Parameters B_2^{d} and $B_3^{^3\mathrm{He}}$ obtained in [28] are compared with the hypertriton $B_3^{^3_\Lambda\mathrm{H}}$ from this analysis using the relations

$$B_2^{^3\mathrm{He}} = \sqrt{\frac{m_{\mathrm{d}}^2}{m_{^3\mathrm{He}}m_{\mathrm{p}}}B_3^{^3\mathrm{He}}} \tag{4}$$

and

$$B_3^{^3_\Lambda\mathrm{H}} = B_3^{^3\mathrm{He}}\frac{m_{\mathrm{p}}m_{^3_\Lambda\mathrm{H}}}{m_{^3\mathrm{He}}m_{\Lambda}}. \tag{5}$$

Finally it is possible to define

$$B_2^{^3_\Lambda\mathrm{H}} = \sqrt{\frac{m_{\mathrm{d}}^2 m_{\Lambda}}{m_{\mathrm{p}}^2 m_{^3_\Lambda\mathrm{H}}}B_3^{^3_\Lambda\mathrm{H}}}. \tag{6}$$

The $B_2^{^3_\Lambda\mathrm{H}}$ parameter evaluated from $B_3^{^3_\Lambda\mathrm{H}}$ is compared in Figure 7 to that of the deuteron, B_2^{d}, and $^3\mathrm{He}$, $B_2^{^3\mathrm{He}}$. The $^3_\Lambda\mathrm{H}$ coalescence parameter is not flat as a function of p_{T} contrary to the prediction of the simple coalescence model [11], which does not take into account the characteristics of the emitting source. This is the same behaviour as observed for deuterons and $^3\mathrm{He}$ nuclei [28]. At low p_{T} the B_2 values are compatible, suggesting that p_0 is similar for A=2 and A=3.

Using the measured $^3_\Lambda\mathrm{H}$ yield the ratio $S_3 = {}^3_\Lambda\mathrm{H}/(^3\mathrm{He}\times\Lambda/\mathrm{p})$, also known as the *Strangeness Population Factor*, [57] was evaluated. This ratio was first suggested by the authors of [8] in the expectation that dividing the strange to non-strange baryon yield should result in a value near unity in a simple coalescence model. Moreover, according to the authors of [57], S_3 is also a valuable tool to probe the nature of the matter created in the collision, since it is sensitive to the local baryon-strangeness correlation [58–60]. This ratio in the thermal model approach does not depend on the chemical potential of particles and was found to be almost energy independent [1, 61]. On the contrary, in a dynamical coalescence picture it increases with decreasing beam energy and is in general larger than the thermal model predictions [61]. This leads to the conclusion that the information on correlations of baryon number and strangeness is lost in the thermal calculation because S_3 essentially depends only on the temperature. On the other hand, in the microscopic treatment the correlation survives and S_3 provides information about the correlation between baryon and strangeness content. Finally, it has been argued [57, 58] that a value of S_3 close to unity indicates that the phase-space populations for strange and light quarks are similar and would support the formation of high-temperature matter of deconfined quarks. The Λ/p ratio used in the present analysis was taken from [50] and [52]. The S_3 values obtained for particles (anti-particles) are summarised in Table 5 and the average of the two measurements is shown in the right panel of Figure 7. These values were compared with different theoretical models and to the results from experiments at BNL-AGS [8] and RHIC [9].

The models used for the comparison are the statistical hadronization model [1], the hybrid UrQMD model [61] and its extension at the LHC energy [49], the DCM (Dubna Cascade Model) coalescence model (described in [61]) and two versions – default and string melting – of the AMPT (A Multi-Phase Transport Model for Relativistic Heavy Ion Collisions) [62] plus coalescence described in [57]. The present result at $\sqrt{s_{\mathrm{NN}}}$ = 2.76 TeV is comparable to that measured at E864 experiment [8] at $\sqrt{s_{\mathrm{NN}}} \sim 5$ GeV, while it does not confirm the rising behaviour shown by STAR [9] and by the AMPT with string melting plus coalescence model [57]. This result is consistent with the thermal model approach, which predicts a constant S_3 value from $\sqrt{s_{\mathrm{NN}}}$ above a few GeV.

5 Conclusions

Measurements of $^3_\Lambda\mathrm{H}$ and $^3_\Lambda\overline{\mathrm{H}}$ in Pb–Pb collisions at $\sqrt{s_{\mathrm{NN}}}$= 2.76 TeV were presented in this letter. The $^3_\Lambda\mathrm{H}$ lifetime was measured and was found to agree with previous measurements within uncertainties. The

Centrality	$\frac{{}^{3}_{\Lambda}\text{H}}{{}^{3}\text{He}} \times \frac{\text{p}}{\Lambda}$	$\frac{{}^{3}_{\Lambda}\overline{\text{H}}}{{}^{3}\overline{\text{He}}} \times \frac{\overline{\text{p}}}{\overline{\Lambda}}$
0–10%	$0.60 \pm 0.13(\text{stat.}) \pm 0.21(\text{syst.})$	$0.54 \pm 0.13(\text{stat.}) \pm 0.19(\text{syst.})$

Table 5: S_3 for matter and anti-matter. To compute the ratio a B.R. of 25% was assumed for the ${}^{3}_{\Lambda}\text{H} \rightarrow {}^{3}\text{He} + \pi$ decay.

Figure 7: Left: B_2 as a function of p_{T} /A for d (full circle) [28], ${}^{3}\text{He}$ (empty circle) [28], and ${}^{3}_{\Lambda}\text{H}$ (full squares). The $B_2^{(\text{d},{}^{3}_{\Lambda}\text{H})}$ and $B_2^{(\text{d},{}^{3}\text{He})}$ were evaluated as explained in the text. $\text{k}_1 = \frac{m_\text{d}^2}{m_{{}^{3}\text{He}} m_\text{p}}$, and $\text{k}_2 = \frac{m_\text{d}^2 m_\Lambda}{m_\text{p}^2 m_{{}^{3}_{\Lambda}\text{H}}}$. Right: S_3 ratio measured in this analysis compared with previous experimental results (E864 [8] and STAR [9] (triangle and star, respectively)) and different theoretical models as indicated in the legend.

measured value was included in the computation of the world average of the ${}^{3}_{\Lambda}\text{H}$ lifetime. Transverse momentum yields at mid-rapidity for central (0–10%) Pb–Pb collisions at $\sqrt{s_{\text{NN}}} = 2.76$ TeV were measured in three p_{T} intervals. The yields of particles and anti-particles were measured in two centrality classes (0–10% and 10–50%) and compared with different theoretical models. The ratio ${}^{3}_{\Lambda}\overline{\text{H}}/{}^{3}_{\Lambda}\text{H}$ is consistent with unity, as expected at the LHC energy. The measured yields indicate that hypernuclei in high-energy heavy-ion collisions are produced within an equilibrated thermal environment in which the temperature is the same as for the other particles produced at the LHC. The ${}^{3}_{\Lambda}\text{H}/{}^{3}\text{He}$ (${}^{3}_{\Lambda}\overline{\text{H}}/{}^{3}\overline{\text{He}}$) ratio was also measured and compared with different theoretical models and results from the STAR experiment. STAR results are higher than ALICE results, but compatible within uncertainties. The ${}^{3}_{\Lambda}\text{H}$ coalescence parameter was also evaluated. Its value increases with p_{T}, and within the uncertainties, is consistent with those extracted for deuteron and ${}^{3}\text{He}$ nuclei [28]. The ratio $S_3 = {}^{3}_{\Lambda}\text{H}/({}^{3}\text{He} \times \Lambda/\text{p})$ was evaluated and compared with different theoretical models and measurements from previous experiments. The value of S_3 suggests that the production of nuclei and hypernuclei at the LHC can be described with a thermodynamic approach, and is similar to the one calculated by the Hybrid UrQMD model [49]. No conclusions can be drawn about the AMPT + coalescence model [57], since no prediction of dynamical coalescence models is available at the LHC energy. The measured S_3 value excludes the rising trend in AMPT seen up to RHIC energies extends to LHC energies. The S_3 measured at AGS, RHIC and LHC are compatible within uncertainty with a value which is independent of the centre of mass energy of the collision.

Acknowledgements

References

[1] A. Andronic, P. Braun-Munzinger, J. Stachel, and H. Stocker, "Production of light nuclei, hypernuclei and their antiparticles in relativistic nuclear collisions,"
Phys.Lett. **B697** (2011) 203–207, arXiv:1010.2995 [nucl-th].

[2] M. Danysz and J. Pniewski, "Delayed Disintegration of a Heavy Nuclear Fragment: I,"
Phil. Mag. **44** (1953) 348–350.

12

[3] F. Weber, R. Negreiros, P. Rosenfield, and A. T. i. Cuadrat, "Neutron star interiors and the equation of state of ultradense matter," *AIP Conf.Proc.* **892** (2007) 515–517, `arXiv:astro-ph/0612132 [astro-ph]`.

[4] H. Heiselberg, "Phases of dense matter in neutron stars," `arXiv:astro-ph/9910200 [astro-ph]`.

[5] I. Vidaña, "Hyperons and neutron stars," *Nucl.Phys.* **A914** (2013) 367–376.

[6] D. Lonardoni, F. Pederiva, and S. Gandolfi, "From hypernuclei to the Inner Core of Neutron Stars: A Quantum Monte Carlo Study," *J.Phys.Conf.Ser.* **529** (2014) 012012, `arXiv:1408.4492 [nucl-th]`.

[7] P. Braun-Munzinger and J. Stachel, "Production of strange clusters and strange matter in nucleus-nucleus collisions at the AGS," *J.Phys.* **G21** (1995) L17–L20, `arXiv:nucl-th/9412035 [nucl-th]`.

[8] **E864** Collaboration, T. Armstrong *et al.*, "Production of ${}^3_\Lambda$H and ${}^4_\Lambda$H in central 11.5-GeV/c Au + Pt heavy ion collisions," *Phys.Rev.* **C70** (2004) 024902, `arXiv:nucl-ex/0211010 [nucl-ex]`.

[9] **STAR** Collaboration, B. Abelev, "Observation of an Antimatter Hypernucleus," *Science* **328** (2010) 58–62, `arXiv:1003.2030 [nucl-ex]`.

[10] **E814** Collaboration, J. Barrette *et al.*, "Production of light nuclei in relativistic heavy ion collisions," *Phys.Rev.* **C50** (1994) 1077–1084.

[11] L. Csernai and J. I. Kapusta, "Entropy and Cluster Production in Nuclear Collisions," *Phys.Rept.* **131** (1986) 223–318.

[12] P. Braun-Munzinger, K. Redlich, and J. Stachel, "Particle production in heavy ion collisions," `arXiv:nucl-th/0304013 [nucl-th]`.

[13] P. Siemens and J. I. Kapusta, "Evidence for a soft nuclear matter equation of state," *Phys.Rev.Lett.* **43** (1979) 1486–1489.

[14] H. Gutbrod, A. Sandoval, P. Johansen, A. M. Poskanzer, J. Gosset, *et al.*, "Final State Interactions in the Production of Hydrogen and Helium Isotopes by Relativistic Heavy Ions on Uranium," *Phys.Rev.Lett.* **37** (1976) 667–670.

[15] J. Steinheimer, M. Mitrovski, T. Schuster, H. Petersen, M. Bleicher, *et al.*, "Strangeness fluctuations and MEMO production at FAIR," *Phys.Lett.* **B676** (2009) 126–131, `arXiv:0811.4077 [hep-ph]`.

[16] **ALICE** Collaboration, B. Abelev *et al.*, "Performance of the ALICE Experiment at the CERN LHC," *Int.J.Mod.Phys.* **A29** (2014) 1430044, `arXiv:1402.4476 [nucl-ex]`.

[17] **ALICE** Collaboration, E. Abbas *et al.*, "Performance of the ALICE VZERO system," *JINST* **8** (2013) P10016, `arXiv:1306.3130 [nucl-ex]`.

[18] **ALICE** Collaboration, K. Aamodt *et al.*, "Centrality dependence of the charged-particle multiplicity density at mid-rapidity in Pb-Pb collisions at $\sqrt{s_{NN}} = 2.76$ TeV," *Phys.Rev.Lett.* **106** (2011) 032301, `arXiv:1012.1657 [nucl-ex]`.

[19] **ALICE** Collaboration, B. Abelev *et al.*, "Centrality determination of Pb-Pb collisions at $\sqrt{s_{NN}} = 2.76$ TeV with ALICE," *Phys.Rev.* **C88** no. 4, (2013) 044909, `arXiv:1301.4361 [nucl-ex]`.

[20] **ALICE** Collaboration, K. Aamodt *et al.*, "Alignment of the ALICE Inner Tracking System with cosmic-ray tracks," *JINST* **5** (2010) P03003, `arXiv:1001.0502 [physics.ins-det]`.

[21] J. Alme, Y. Andres, H. Appelshäuser, S. Bablok, N. Bialas, *et al.*, "The ALICE TPC, a large 3-dimensional tracking device with fast readout for ultra-high multiplicity events," *Nucl.Instrum.Meth.* **A622** (2010) 316–367, `arXiv:1001.1950 [physics.ins-det]`.

[22] M. Juric, G. Bohm, J. Klabuhn, U. Krecker, F. Wysotzki, *et al.*, "A new determination of the binding-energy values of the light hypernuclei (A ≤15)," *Nucl.Phys.* **B52** (1973) 1–30.

[23] X.-N. Wang and M. Gyulassy, "HIJING: A Monte Carlo model for multiple jet production in p p,

p A and A A collisions," *Phys.Rev.* **D44** (1991) 3501–3516.

[24] R. Brun, F. Carminati, and S. Giani, "GEANT Detector Description and Simulation Tool," *Program Library Long Write-up W5013* (1994) .

[25] H. Bando, T. Motoba, and J. Zofka, "Production, structure and decay of hypernuclei," *Int.J.Mod.Phys.* **A5** (1990) 4021–4198.

[26] **ALICE** Collaboration, B. Abelev *et al.*, "Centrality Dependence of Charged Particle Production at Large Transverse Momentum in Pb–Pb Collisions at $\sqrt{s_{\text{NN}}} = 2.76$ TeV," *Phys.Lett.* **B720** (2013) 52–62, arXiv:1208.2711 [hep-ex].

[27] E. Schnedermann, J. Sollfrank, and U. W. Heinz, "Thermal phenomenology of hadrons from 200A GeV S+S collisions," *Phys.Rev.* **C48** (1993) 2462–2475, arXiv:nucl-th/9307020 [nucl-th].

[28] **ALICE** Collaboration, J. Adam *et al.*, "Measurement of light nuclei and anti-nuclei in pp and PbPb collisions at LHC energies," *In preparation* (2015) .

[29] R. Brun and F. Rademakers, "ROOT: An object oriented data analysis framework," *Nucl.Instrum.Meth.* **A389** (1997) 81–86.

[30] **Particle Data Group** Collaboration, K. Olive *et al.*, "Review of Particle Physics," *Chin.Phys.* **C38** (2014) 090001.

[31] H. Kamada, J. Golak, K. Miyagawa, H. Witala, and W. Gloeckle, "Pi mesonic decay of the hypertriton," *Phys.Rev.* **C57** (1998) 1595–1603, arXiv:nucl-th/9709035 [nucl-th].

[32] R. J. Prem and P. H. Steinberg, "Lifetimes of Hypernuclei, $^{3}_{\Lambda}$H,$^{4}_{\Lambda}$H,$^{5}_{\Lambda}$H," *Phys. Rev.* **136** (1964) B1803–B1806.

[33] G. Keyes, M. Derrick, T. Fields, L. Hyman, J. Fetkovich, *et al.*, "New Measurement of the $^{3}_{\Lambda}$H Lifetime," *Phys.Rev.Lett.* **20** (1968) 819–821.

[34] R. Phillips and J. Schneps, "Lifetimes of light hyperfragments. ii," *Phys.Rev.* **180** (1969) 1307–1318.

[35] G. Bohm, J. Klabuhn, U. Krecker, F. Wysotzki, G. Coremans, *et al.*, "On the lifetime of the $^{3}_{\Lambda}$H hypernucleus," *Nucl.Phys.* **B16** (1970) 46–52.

[36] G. Keyes, M. Derrick, T. Fields, L. Hyman, J. Fetkovich, *et al.*, "Properties of $^{3}_{\Lambda}$H," *Phys.Rev.* **D1** (1970) 66–77.

[37] G. Keyes, J. Sacton, J. Wickens, and M. Block, "A measurement of the lifetime of the $^{3}_{\Lambda}$H hypernucleus," *Nucl.Phys.* **B67** (1973) 269–283.

[38] C. Rappold, E. Kim, D. Nakajima, T. Saito, O. Bertini, *et al.*, "Hypernuclear spectroscopy of products from ^{6}Li projectiles on a carbon target at 2 AGeV," *Nucl.Phys.* **A913** (2013) 170–184, arXiv:1305.4871 [nucl-ex].

[39] R. Dalitz and L. Liu, "Pionic Decay Modes of Light Lambda Hypernuclei," *Phys.Rev.* **116** (1959) 1312–1321.

[40] R. Dalitz and G. Rajasekharan, "The spins and lifetimes of the light hypernuclei," *Phys.Lett.* **1** (1962) 58–60.

[41] M. Rayet and R. Dalitz, "Lifetime of $^{3}_{\Lambda}$H," *Nuovo Cim.* **A46** (1966) 786–794.

[42] B. Ram and W. Williams, "Decay rate and branching ratio (π^{-} ^{3}He)/(all π^{-} modes) of $^{3}_{\Lambda}$H," *Nucl.Phys.* **B28** (1971) 566–572.

[43] H. Mansour and K. Higgins, "The decay rate of $^{3}_{\Lambda}$H," *Nuovo Cim.* **A51** (1979) 180–186.

[44] N. Kolesnikov and V. Kopylov, "Meson decays of hypertritium," *Sov.Phys.J.* **31** (1988) 210–213.

[45] J. Congleton, "A Simple model of the hypertriton," *J.Phys.* **G18** (1992) 339–357.

[46] W. Gloeckle, K. Miyagawa, H. Kamada, J. Golak, and H. Witala, "The hypertriton and its decays," *Nucl.Phys.* **A639** (1998) 297–306.

[47] C. Rappold, T. Saito, O. Bertini, S. Bianchin, V. Bozkurt, *et al.*, "On the measured lifetime of light

hypernuclei ${}^{3}_{\Lambda}$H and ${}^{4}_{\Lambda}$H," *Phys.Lett.* **B728** (2014) 543–548.

[48] M. Petráň, J. Letessier, V. Petráček, and J. Rafelski, "Hadron production and quark-gluon plasma hadronization in Pb-Pb collisions at $\sqrt{s_{NN}} = 2.76$ TeV," *Phys.Rev.* **C88** no. 3, (2013) 034907, `arXiv:1303.2098 [hep-ph]`.

[49] J. Steinheimer. Calculation based on [61] (2015).

[50] **ALICE** Collaboration, B. Abelev *et al.*, "Centrality dependence of π, K, p production in Pb-Pb collisions at $\sqrt{s_{NN}} = 2.76$ TeV," *Phys.Rev.* **C88** (2013) 044910, `arXiv:1303.0737 [hep-ex]`.

[51] **ALICE** Collaboration, B. Abelev *et al.*, "Multi-strange baryon production at mid-rapidity in Pb-Pb collisions at $\sqrt{s_{NN}} = 2.76$ TeV," *Phys.Lett.* **B728** (2014) 216–227, `arXiv:1307.5543 [nucl-ex]`.

[52] **ALICE** Collaboration, B. Abelev *et al.*, "K^{0}_{S} and Λ production in Pb-Pb collisions at $\sqrt{s_{NN}} = 2.76$ TeV," *Phys.Rev.Lett.* **111** (2013) 222301, `arXiv:1307.5530 [nucl-ex]`.

[53] **ALICE** Collaboration, B. Abelev *et al.*, "$K^{*}(892)^{0}$ and $\phi(1020)$ production in Pb-Pb collisions at $\sqrt{s_{NN}} = 2.76$ TeV," *Phys.Rev.* **C91** (2015) 024609, `arXiv:1404.0495 [nucl-ex]`.

[54] M. Floris, "Hadron yields and the phase diagram of strongly interacting matter," *Nucl.Phys.* **A931** (2014) 103–112, `arXiv:1408.6403 [nucl-ex]`.

[55] J. Cleymans, S. Kabana, I. Kraus, H. Oeschler, K. Redlich, *et al.*, "Antimatter production in proton-proton and heavy-ion collisions at ultrarelativistic energies," *Phys.Rev.* **C84** (2011) 054916, `arXiv:1105.3719 [hep-ph]`.

[56] S. Pal and W. Greiner, "Production of antinuclei and hypernuclei in a relativistic Hagedorn resonance gas model," *Phys.Rev.* **C87** no. 5, (2013) 054905.

[57] S. Zhang, J. Chen, H. Crawford, D. Keane, Y. Ma, *et al.*, "Searching for onset of deconfinement via hypernuclei and baryon-strangeness correlations," *Phys.Lett.* **B684** (2010) 224–227, `arXiv:0908.3357 [nucl-ex]`.

[58] V. Koch, A. Majumder, and J. Randrup, "Baryon-strangeness correlations: A Diagnostic of strongly interacting matter," *Phys.Rev.Lett.* **95** (2005) 182301, `arXiv:nucl-th/0505052 [nucl-th]`.

[59] A. Majumder and B. Muller, "Baryonic strangeness and related susceptibilities in QCD," *Phys.Rev.* **C74** (2006) 054901, `arXiv:nucl-th/0605079 [nucl-th]`.

[60] M. Cheng, P. Hegde, C. Jung, F. Karsch, O. Kaczmarek, *et al.*, "Baryon Number, Strangeness and Electric Charge Fluctuations in QCD at High Temperature," *Phys.Rev.* **D79** (2009) 074505, `arXiv:0811.1006 [hep-lat]`.

[61] J. Steinheimer, K. Gudima, A. Botvina, I. Mishustin, M. Bleicher, *et al.*, "Hypernuclei, dibaryon and antinuclei production in high energy heavy ion collisions: Thermal production versus Coalescence," *Phys.Lett.* **B714** (2012) 85–91, `arXiv:1203.2547 [nucl-th]`.

[62] Z.-W. Lin, C. M. Ko, B.-A. Li, B. Zhang, and S. Pal, "A Multi-phase transport model for relativistic heavy ion collisions," *Phys.Rev.* **C72** (2005) 064901, `arXiv:nucl-th/0411110 [nucl-th]`.

A   The ALICE Collaboration

J. Adam[40], D. Adamová[83], M.M. Aggarwal[87], G. Aglieri Rinella[36], M. Agnello[111], N. Agrawal[48], Z. Ahammed[132], S.U. Ahn[68], I. Aimo[94 ,111], S. Aiola[137], M. Ajaz[16], A. Akindinov[58], S.N. Alam[132], D. Aleksandrov[100], B. Alessandro[111], D. Alexandre[102], R. Alfaro Molina[64], A. Alici[105 ,12], A. Alkin[3], J. Alme[38], T. Alt[43], S. Altinpinar[18], I. Altsybeev[131], C. Alves Garcia Prado[120], C. Andrei[78], A. Andronic[97], V. Anguelov[93], J. Anielski[54], T. Antičić[98], F. Antinori[108], P. Antonioli[105], L. Aphecetche[113], H. Appelshäuser[53], S. Arcelli[28], N. Armesto[17], R. Arnaldi[111], I.C. Arsene[22], M. Arslandok[53], B. Audurier[113], A. Augustinus[36], R. Averbeck[97], M.D. Azmi[19], M. Bach[43], A. Badalà[107], Y.W. Baek[44], S. Bagnasco[111], R. Bailhache[53], R. Bala[90], A. Baldisseri[15], F. Baltasar Dos Santos Pedrosa[36], R.C. Baral[61], A.M. Barbano[111], R. Barbera[29], F. Barile[33], G.G. Barnaföldi[136], L.S. Barnby[102], V. Barret[70], P. Bartalini[7], K. Barth[36], J. Bartke[117], E. Bartsch[53], M. Basile[28], N. Bastid[70], S. Basu[132], B. Bathen[54], G. Batigne[113], A. Batista Camejo[70], B. Batyunya[66], P.C. Batzing[22], I.G. Bearden[80], H. Beck[53], C. Bedda[111], N.K. Behera[49 ,48], I. Belikov[55], F. Bellini[28], H. Bello Martinez[2], R. Bellwied[122], R. Belmont[135], E. Belmont-Moreno[64], V. Belyaev[76], G. Bencedi[136], S. Beole[27], I. Berceanu[78], A. Bercuci[78], Y. Berdnikov[85], D. Berenyi[136], R.A. Bertens[57], D. Berzano[36 ,27], L. Betev[36], A. Bhasin[90], I.R. Bhat[90], A.K. Bhati[87], B. Bhattacharjee[45], J. Bhom[128], L. Bianchi[122], N. Bianchi[72], C. Bianchin[135 ,57], J. Bielčík[40], J. Bielčíková[83], A. Bilandzic[80], R. Biswas[4], S. Biswas[79], S. Bjelogrlic[57], F. Blanco[10], D. Blau[100], C. Blume[53], F. Bock[74 ,93], A. Bogdanov[76], H. Bøggild[80], L. Boldizsár[136], M. Bombara[41], J. Book[53], H. Borel[15], A. Borissov[96], M. Borri[82], F. Bossú[65], M. Botje[81], E. Botta[27], S. Böttger[52], P. Braun-Munzinger[97], M. Bregant[120], T. Breitner[52], T.A. Broker[53], T.A. Browning[95], M. Broz[40], E.J. Brucken[46], E. Bruna[111], G.E. Bruno[33], D. Budnikov[99], H. Buesching[53], S. Bufalino[111 ,36], P. Buncic[36], O. Busch[93 ,128], Z. Buthelezi[65], J.T. Buxton[20], D. Caffarri[36], X. Cai[7], H. Caines[137], L. Calero Diaz[72], A. Caliva[57], E. Calvo Villar[103], P. Camerini[26], F. Carena[36], W. Carena[36], J. Castillo Castellanos[15], A.J. Castro[125], E.A.R. Casula[25], C. Cavicchioli[36], C. Ceballos Sanchez[9], J. Cepila[40], P. Cerello[111], J. Cerkala[115], B. Chang[123], S. Chapeland[36], M. Chartier[124], J.L. Charvet[15], S. Chattopadhyay[132], S. Chattopadhyay[101], V. Chelnokov[3], M. Cherney[86], C. Cheshkov[130], B. Cheynis[130], V. Chibante Barroso[36], D.D. Chinellato[121], P. Chochula[36], K. Choi[96], M. Chojnacki[80], S. Choudhury[132], P. Christakoglou[81], C.H. Christensen[80], P. Christiansen[34], T. Chujo[128], S.U. Chung[96], Z. Chunhui[57], C. Cicalo[106], L. Cifarelli[12 ,28], F. Cindolo[105], J. Cleymans[89], F. Colamaria[33], D. Colella[33 ,59], A. Collu[25], M. Colocci[28], G. Conesa Balbastre[71], Z. Conesa del Valle[51], M.E. Connors[137], J.G. Contreras[11 ,40], T.M. Cormier[84], Y. Corrales Morales[27], I. Cortés Maldonado[2], P. Cortese[32], M.R. Cosentino[120], F. Costa[36], P. Crochet[70], R. Cruz Albino[11], E. Cuautle[63], L. Cunqueiro[36], T. Dahms[92 ,37], A. Dainese[108], A. Danu[62], D. Das[101], I. Das[51 ,101], S. Das[4], A. Dash[121], S. Dash[48], S. De[120], A. De Caro[31 ,12], G. de Cataldo[104], J. de Cuveland[43], A. De Falco[25], D. De Gruttola[12 ,31], N. De Marco[111], S. De Pasquale[31], A. Deisting[97 ,93], A. Deloff[77], E. Dénes[136], G. D'Erasmo[33], D. Di Bari[33], A. Di Mauro[36], P. Di Nezza[72], M.A. Diaz Corchero[10], T. Dietel[89], P. Dillenseger[53], R. Divià[36], Ø. Djuvsland[18], A. Dobrin[57 ,81], T. Dobrowolski[77 ,i], D. Domenicis Gimenez[120], B. Dönigus[53], O. Dordic[22], A.K. Dubey[132], A. Dubla[57], L. Ducroux[130], P. Dupieux[70], R.J. Ehlers[137], D. Elia[104], H. Engel[52], B. Erazmus[36 ,113], I. Erdemir[53], F. Erhardt[129], D. Eschweiler[43], B. Espagnon[51], M. Estienne[113], S. Esumi[128], J. Eum[96], D. Evans[102], S. Evdokimov[112], G. Eyyubova[40], L. Fabbietti[37 ,92], D. Fabris[108], J. Faivre[71], A. Fantoni[72], M. Fasel[74], L. Feldkamp[54], D. Felea[62], A. Feliciello[111], G. Feofilov[131], J. Ferencei[83], A. Fernández Téllez[2], E.G. Ferreiro[17], A. Ferretti[27], A. Festanti[30], V.J.G. Feuillard[70 ,15], J. Figiel[117], M.A.S. Figueredo[124], S. Filchagin[99], D. Finogeev[56], F.M. Fionda[104], E.M. Fiore[33], M.G. Fleck[93], M. Floris[36], S. Foertsch[65], P. Foka[97], S. Fokin[100], E. Fragiacomo[110], A. Francescon[30 ,36], U. Frankenfeld[97], U. Fuchs[36], C. Furget[71], A. Furs[56], M. Fusco Girard[31], J.J. Gaardhøje[80], M. Gagliardi[27], A.M. Gago[103], M. Gallio[27], D.R. Gangadharan[74], P. Ganoti[88], C. Gao[7], C. Garabatos[97], E. Garcia-Solis[13], C. Gargiulo[36], P. Gasik[92 ,37], M. Germain[113], A. Gheata[36], M. Gheata[62 ,36], P. Ghosh[132], S.K. Ghosh[4], P. Gianotti[72], P. Giubellino[36], P. Giubilato[30], E. Gladysz-Dziadus[117], P. Glässel[93], A. Gomez Ramirez[52], P. González-Zamora[10], S. Gorbunov[43], L. Görlich[117], S. Gotovac[116], V. Grabski[64], L.K. Graczykowski[134], K.L. Graham[102], A. Grelli[57], A. Grigoras[36], C. Grigoras[36], V. Grigoriev[76], A. Grigoryan[1], S. Grigoryan[66], B. Grinyov[3], N. Grion[110], J.F. Grosse-Oetringhaus[36], J.-Y. Grossiord[130], R. Grosso[36], F. Guber[56], R. Guernane[71], B. Guerzoni[28], K. Gulbrandsen[80], H. Gulkanyan[1], T. Gunji[127], A. Gupta[90], R. Gupta[90], R. Haake[54], Ø. Haaland[18], C. Hadjidakis[51], M. Haiduc[62], H. Hamagaki[127], G. Hamar[136], A. Hansen[80], J.W. Harris[137], H. Hartmann[43], A. Harton[13], D. Hatzifotiadou[105], S. Hayashi[127], S.T. Heckel[53], M. Heide[54], H. Helstrup[38], A. Herghelegiu[78], G. Herrera Corral[11], B.A. Hess[35], K.F. Hetland[38], T.E. Hilden[46], H. Hillemanns[36], B. Hippolyte[55], R. Hosokawa[128], P. Hristov[36], M. Huang[18], T.J. Humanic[20], N. Hussain[45], T. Hussain[19], D. Hutter[43], D.S. Hwang[21], R. Ilkaev[99], I. Ilkiv[77], M. Inaba[128], C. Ionita[36], M. Ippolitov[76 ,100], M. Irfan[19], M. Ivanov[97], V. Ivanov[85], V. Izucheev[112], P.M. Jacobs[74], S. Jadlovska[115], C. Jahnke[120],

H.J. Jang[68] , M.A. Janik[134] , P.H.S.Y. Jayarathna[122] , C. Jena[30] , S. Jena[122] , R.T. Jimenez Bustamante[97] ,
P.G. Jones[102] , H. Jung[44] , A. Jusko[102] , P. Kalinak[59] , A. Kalweit[36] , J. Kamin[53] , J.H. Kang[138] , V. Kaplin[76] ,
S. Kar[132] , A. Karasu Uysal[69] , O. Karavichev[56] , T. Karavicheva[56] , E. Karpechev[56] , U. Kebschull[52] ,
R. Keidel[139] , D.L.D. Keijdener[57] , M. Keil[36] , K.H. Khan[16] , M.M. Khan[19] , P. Khan[101] , S.A. Khan[132] ,
A. Khanzadeev[85] , Y. Kharlov[112] , B. Kileng[38] , B. Kim[138] , D.W. Kim[44 ,68] , D.J. Kim[123] , H. Kim[138] ,
J.S. Kim[44] , M. Kim[44] , M. Kim[138] , S. Kim[21] , T. Kim[138] , S. Kirsch[43] , I. Kisel[43] , S. Kiselev[58] , A. Kisiel[134] ,
G. Kiss[136] , J.L. Klay[6] , C. Klein[53] , J. Klein[93] , C. Klein-Bösing[54] , A. Kluge[36] , M.L. Knichel[93] ,
A.G. Knospe[118] , T. Kobayashi[128] , C. Kobdaj[114] , M. Kofarago[36] , T. Kollegger[97 ,43] , A. Kolojvari[131] ,
V. Kondratiev[131] , N. Kondratyeva[76] , E. Kondratyuk[112] , A. Konevskikh[56] , M. Kopcik[115] , C. Kouzinopoulos[36] ,
O. Kovalenko[77] , V. Kovalenko[131] , M. Kowalski[117] , S. Kox[71] , G. Koyithatta Meethaleveedu[48] , J. Kral[123] ,
I. Králik[59] , A. Kravčáková[41] , M. Krelina[40] , M. Kretz[43] , M. Krivda[102 ,59] , F. Krizek[83] , E. Kryshen[36] ,
M. Krzewicki[43] , A.M. Kubera[20] , V. Kučera[83] , T. Kugathasan[36] , C. Kuhn[55] , P.G. Kuijer[81] , I. Kulakov[43] ,
J. Kumar[48] , L. Kumar[79 ,87] , P. Kurashvili[77] , A. Kurepin[56] , A.B. Kurepin[56] , A. Kuryakin[99] , S. Kushpil[83] ,
M.J. Kweon[50] , Y. Kwon[138] , S.L. La Pointe[111] , P. La Rocca[29] , C. Lagana Fernandes[120] , I. Lakomov[36] ,
R. Langoy[42] , C. Lara[52] , A. Lardeux[15] , A. Lattuca[27] , E. Laudi[36] , R. Lea[26] , L. Leardini[93] , G.R. Lee[102] ,
S. Lee[138] , I. Legrand[36] , R.C. Lemmon[82] , V. Lenti[104] , E. Leogrande[57] , I. León Monzón[119] , M. Leoncino[27] ,
P. Lévai[136] , S. Li[7 ,70] , X. Li[14] , J. Lien[42] , R. Lietava[102] , S. Lindal[22] , V. Lindenstruth[43] , C. Lippmann[97] ,
M.A. Lisa[20] , H.M. Ljunggren[34] , D.F. Lodato[57] , P.I. Loenne[18] , V.R. Loggins[135] , V. Loginov[76] , C. Loizides[74] ,
X. Lopez[70] , E. López Torres[9] , A. Lowe[136] , P. Luettig[53] , M. Lunardon[30] , G. Luparello[26] , P.H.F.N.D. Luz[120] ,
A. Maevskaya[56] , M. Mager[36] , S. Mahajan[90] , S.M. Mahmood[22] , A. Maire[55] , R.D. Majka[137] , M. Malaev[85] ,
I. Maldonado Cervantes[63] , L. Malinina[66] , D. Mal'Kevich[58] , P. Malzacher[97] , A. Mamonov[99] , L. Manceau[111] ,
V. Manko[100] , F. Manso[70] , V. Manzari[36 ,104] , M. Marchisone[27] , J. Mareš[60] , G.V. Margagliotti[26] ,
A. Margotti[105] , J. Margutti[57] , A. Marín[97] , C. Markert[118] , M. Marquard[53] , N.A. Martin[97] , J. Martin Blanco[113] ,
P. Martinengo[36] , M.I. Martínez[2] , G. Martínez García[113] , M. Martinez Pedreira[36] , Y. Martynov[3] , A. Mas[120] ,
S. Masciocchi[97] , M. Masera[27] , A. Masoni[106] , L. Massacrier[113] , A. Mastroserio[33] , H. Masui[128] , A. Matyja[117] ,
C. Mayer[117] , J. Mazer[125] , M.A. Mazzoni[109] , D. Mcdonald[122] , F. Meddi[24] , A. Menchaca-Rocha[64] ,
E. Meninno[31] , J. Mercado Pérez[93] , M. Meres[39] , Y. Miake[128] , M.M. Mieskolainen[46] , K. Mikhaylov[58 ,66] ,
L. Milano[36] , J. Milosevic[22 ,133] , L.M. Minervini[23 ,104] , A. Mischke[57] , A.N. Mishra[49] , D. Miśkowiec[97] ,
J. Mitra[132] , C.M. Mitu[62] , N. Mohammadi[57] , B. Mohanty[79 ,132] , L. Molnar[55] , L. Montaño Zetina[11] ,
E. Montes[10] , M. Morando[30] , D.A. Moreira De Godoy[113 ,54] , S. Moretto[30] , A. Morreale[113] , A. Morsch[36] ,
V. Muccifora[72] , E. Mudnic[116] , D. Mühlheim[54] , S. Muhuri[132] , M. Mukherjee[132] , J.D. Mulligan[137] ,
M.G. Munhoz[120] , S. Murray[65] , L. Musa[36] , J. Musinsky[59] , B.K. Nandi[48] , R. Nania[105] , E. Nappi[104] ,
M.U. Naru[16] , C. Nattrass[125] , K. Nayak[79] , T.K. Nayak[132] , S. Nazarenko[99] , A. Nedosekin[58] , L. Nellen[63] ,
F. Ng[122] , M. Nicassio[97] , M. Niculescu[62 ,36] , J. Niedziela[36] , B.S. Nielsen[80] , S. Nikolaev[100] , S. Nikulin[100] ,
V. Nikulin[85] , F. Noferini[12 ,105] , P. Nomokonov[66] , G. Nooren[57] , J.C.C. Noris[2] , J. Norman[124] , A. Nyanin[100] ,
J. Nystrand[18] , H. Oeschler[93] , S. Oh[137] , S.K. Oh[67] , A. Ohlson[36] , A. Okatan[69] , T. Okubo[47] , L. Olah[136] ,
J. Oleniacz[134] , A.C. Oliveira Da Silva[120] , M.H. Oliver[137] , J. Onderwaater[97] , C. Oppedisano[111] , A. Ortiz
Velasquez[63] , A. Oskarsson[34] , J. Otwinowski[117] , K. Oyama[93] , M. Ozdemir[53] , Y. Pachmayr[93] , P. Pagano[31] ,
G. Paić[63] , C. Pajares[17] , S.K. Pal[132] , J. Pan[135] , A.K. Pandey[48] , D. Pant[48] , P. Papcun[115] , V. Papikyan[1] ,
G.S. Pappalardo[107] , P. Pareek[49] , W.J. Park[97] , S. Parmar[87] , A. Passfeld[54] , V. Paticchio[104] , R.N. Patra[132] ,
B. Paul[101] , T. Peitzmann[57] , H. Pereira Da Costa[15] , E. Pereira De Oliveira Filho[120] , D. Peresunko[76 ,100] ,
C.E. Pérez Lara[81] , V. Peskov[53] , Y. Pestov[5] , V. Petráček[40] , V. Petrov[112] , M. Petrovici[78] , C. Petta[29] , S. Piano[110] ,
M. Pikna[39] , P. Pillot[113] , O. Pinazza[105 ,36] , L. Pinsky[122] , D.B. Piyarathna[122] , M. Płoskoń[74] , M. Planinic[129] ,
J. Pluta[134] , S. Pochybova[136] , P.L.M. Podesta-Lerma[119] , M.G. Poghosyan[86] , B. Polichtchouk[112] , N. Poljak[129] ,
W. Poonsawat[114] , A. Pop[78] , S. Porteboeuf-Houssais[70] , J. Porter[74] , J. Pospisil[83] , S.K. Prasad[4] ,
R. Preghenella[105 ,36] , F. Prino[111] , C.A. Pruneau[135] , I. Pshenichnov[56] , M. Puccio[111] , G. Puddu[25] ,
P. Pujahari[135] , V. Punin[99] , J. Putschke[135] , H. Qvigstad[22] , A. Rachevski[110] , S. Raha[4] , S. Rajput[90] , J. Rak[123] ,
A. Rakotozafindrabe[15] , L. Ramello[32] , R. Raniwala[91] , S. Raniwala[91] , S.S. Räsänen[46] , B.T. Rascanu[53] ,
D. Rathee[87] , K.F. Read[125] , J.S. Real[71] , K. Redlich[77] , R.J. Reed[135] , A. Rehman[18] , P. Reichelt[53] , F. Reidt[93 ,36] ,
X. Ren[7] , R. Renfordt[53] , A.R. Reolon[72] , A. Reshetin[56] , F. Rettig[43] , J.-P. Revol[12] , K. Reygers[93] , V. Riabov[85] ,
R.A. Ricci[73] , T. Richert[34] , M. Richter[22] , P. Riedler[36] , W. Riegler[36] , F. Riggi[29] , C. Ristea[62] , A. Rivetti[111] ,
E. Rocco[57] , M. Rodríguez Cahuantzi[2] , A. Rodriguez Manso[81] , K. Røed[22] , E. Rogochaya[66] , D. Rohr[43] ,
D. Röhrich[18] , R. Romita[124] , F. Ronchetti[72] , L. Ronflette[113] , P. Rosnet[70] , A. Rossi[36 ,30] , F. Roukoutakis[88] ,
A. Roy[49] , C. Roy[55] , P. Roy[101] , A.J. Rubio Montero[10] , R. Rui[26] , R. Russo[27] , E. Ryabinkin[100] , Y. Ryabov[85] ,
A. Rybicki[117] , S. Sadovsky[112] , K. Šafařík[36] , B. Sahlmuller[53] , P. Sahoo[49] , R. Sahoo[49] , S. Sahoo[61] ,
P.K. Sahu[61] , J. Saini[132] , S. Sakai[72] , M.A. Saleh[135] , C.A. Salgado[17] , J. Salzwedel[20] , S. Sambyal[90] ,

V. Samsonov[85], X. Sanchez Castro[55], L. Šándor[59], A. Sandoval[64], M. Sano[128], G. Santagati[29], D. Sarkar[132], E. Scapparone[105], F. Scarlassara[30], R.P. Scharenberg[95], C. Schiaua[78], R. Schicker[93], C. Schmidt[97], H.R. Schmidt[35], S. Schuchmann[53], J. Schukraft[36], M. Schulc[40], T. Schuster[137], Y. Schutz[113,36], K. Schwarz[97], K. Schweda[97], G. Scioli[28], E. Scomparin[111], R. Scott[125], K.S. Seeder[120], J.E. Seger[86], Y. Sekiguchi[127], D. Sekihata[47], I. Selyuzhenkov[97], K. Senosi[65], J. Seo[96,67], E. Serradilla[64,10], A. Sevcenco[62], A. Shabanov[56], A. Shabetai[113], O. Shadura[3], R. Shahoyan[36], A. Shangaraev[112], A. Sharma[90], N. Sharma[61,125], K. Shigaki[47], K. Shtejer[9,27], Y. Sibiriak[100], S. Siddhanta[106], K.M. Sielewicz[36], T. Siemiarczuk[77], D. Silvermyr[84,34], C. Silvestre[71], G. Simatovic[129], G. Simonetti[36], R. Singaraju[132], R. Singh[79], S. Singha[79,132], V. Singhal[132], B.C. Sinha[132], T. Sinha[101], B. Sitar[39], M. Sitta[32], T.B. Skaali[22], M. Slupecki[123], N. Smirnov[137], R.J.M. Snellings[57], T.W. Snellman[123], C. Søgaard[34], R. Soltz[75], J. Song[96], M. Song[138], Z. Song[7], F. Soramel[30], S. Sorensen[125], M. Spacek[40], E. Spiriti[72], I. Sputowska[117], M. Spyropoulou-Stassinaki[88], B.K. Srivastava[95], J. Stachel[93], I. Stan[62], G. Stefanek[77], M. Steinpreis[20], E. Stenlund[34], G. Steyn[65], J.H. Stiller[93], D. Stocco[113], P. Strmen[39], A.A.P. Suaide[120], T. Sugitate[47], C. Suire[51], M. Suleymanov[16], R. Sultanov[58], M. Šumbera[83], T.J.M. Symons[74], A. Szabo[39], A. Szanto de Toledo[120,i], I. Szarka[39], A. Szczepankiewicz[36], M. Szymanski[134], J. Takahashi[121], N. Tanaka[128], M.A. Tangaro[33], J.D. Tapia Takaki[ii,51], A. Tarantola Peloni[53], M. Tarhini[51], M. Tariq[19], M.G. Tarzila[78], A. Tauro[36], G. Tejeda Muñoz[2], A. Telesca[36], K. Terasaki[127], C. Terrevoli[30,25], B. Teyssier[130], J. Thäder[74,97], D. Thomas[118], R. Tieulent[130], A.R. Timmins[122], A. Toia[53], S. Trogolo[111], V. Trubnikov[3], W.H. Trzaska[123], T. Tsuji[127], A. Tumkin[99], R. Turrisi[108], T.S. Tveter[22], K. Ullaland[18], A. Uras[130], G.L. Usai[25], A. Utrobicic[129], M. Vajzer[83], M. Vala[59], L. Valencia Palomo[70], S. Vallero[27], J. Van Der Maarel[57], J.W. Van Hoorne[36], M. van Leeuwen[57], T. Vanat[83], P. Vande Vyvre[36], D. Varga[136], A. Vargas[2], M. Vargyas[123], R. Varma[48], M. Vasileiou[88], A. Vasiliev[100], A. Vauthier[71], V. Vechernin[131], A.M. Veen[57], M. Veldhoen[57], A. Velure[18], M. Venaruzzo[73], E. Vercellin[27], S. Vergara Limón[2], R. Vernet[8], M. Verweij[135], L. Vickovic[116], G. Viesti[30,i], J. Viinikainen[123], Z. Vilakazi[126], O. Villalobos Baillie[102], A. Vinogradov[100], L. Vinogradov[131], Y. Vinogradov[99,i], T. Virgili[31], V. Vislavicius[34], Y.P. Viyogi[132], A. Vodopyanov[66], M.A. Völkl[93], K. Voloshin[58], S.A. Voloshin[135], G. Volpe[136,36], B. von Haller[36], I. Vorobyev[92,37], D. Vranic[97,36], J. Vrláková[41], B. Vulpescu[70], A. Vyushin[99], B. Wagner[18], J. Wagner[97], H. Wang[57], M. Wang[7,113], Y. Wang[93], D. Watanabe[128], Y. Watanabe[127], M. Weber[36], S.G. Weber[97], J.P. Wessels[54], U. Westerhoff[54], J. Wiechula[35], J. Wikne[22], M. Wilde[54], G. Wilk[77], J. Wilkinson[93], M.C.S. Williams[105], B. Windelband[93], M. Winn[93], C.G. Yaldo[135], H. Yang[57], P. Yang[7], S. Yano[47], Z. Yin[7], H. Yokoyama[128], I.-K. Yoo[96], V. Yurchenko[3], I. Yushmanov[100], A. Zaborowska[134], V. Zaccolo[80], A. Zaman[16], C. Zampolli[105], H.J.C. Zanoli[120], S. Zaporozhets[66], N. Zardoshti[102], A. Zarochentsev[131], P. Závada[60], N. Zaviyalov[99], H. Zbroszczyk[134], I.S. Zgura[62], M. Zhalov[85], H. Zhang[18,7], X. Zhang[74], Y. Zhang[7], C. Zhao[22], N. Zhigareva[58], D. Zhou[7], Y. Zhou[80,57], Z. Zhou[18], H. Zhu[18,7], J. Zhu[113,7], X. Zhu[7], A. Zichichi[12,28], A. Zimmermann[93], M.B. Zimmermann[54,36], G. Zinovjev[3], M. Zyzak[43]

Affiliation notes

[i] Deceased

[ii] Also at: University of Kansas, Lawrence, Kansas, United States

Collaboration Institutes

[1] A.I. Alikhanyan National Science Laboratory (Yerevan Physics Institute) Foundation, Yerevan, Armenia

[2] Benemérita Universidad Autónoma de Puebla, Puebla, Mexico

[3] Bogolyubov Institute for Theoretical Physics, Kiev, Ukraine

[4] Bose Institute, Department of Physics and Centre for Astroparticle Physics and Space Science (CAPSS), Kolkata, India

[5] Budker Institute for Nuclear Physics, Novosibirsk, Russia

[6] California Polytechnic State University, San Luis Obispo, California, United States

[7] Central China Normal University, Wuhan, China

[8] Centre de Calcul de l'IN2P3, Villeurbanne, France

[9] Centro de Aplicaciones Tecnológicas y Desarrollo Nuclear (CEADEN), Havana, Cuba

[10] Centro de Investigaciones Energéticas Medioambientales y Tecnológicas (CIEMAT), Madrid, Spain

[11] Centro de Investigación y de Estudios Avanzados (CINVESTAV), Mexico City and Mérida, Mexico

[12] Centro Fermi - Museo Storico della Fisica e Centro Studi e Ricerche "Enrico Fermi", Rome, Italy

[13] Chicago State University, Chicago, Illinois, USA

[14] China Institute of Atomic Energy, Beijing, China

[15] Commissariat à l'Energie Atomique, IRFU, Saclay, France

[16] COMSATS Institute of Information Technology (CIIT), Islamabad, Pakistan

[17] Departamento de Física de Partículas and IGFAE, Universidad de Santiago de Compostela, Santiago de Compostela, Spain

[18] Department of Physics and Technology, University of Bergen, Bergen, Norway

[19] Department of Physics, Aligarh Muslim University, Aligarh, India

[20] Department of Physics, Ohio State University, Columbus, Ohio, United States

[21] Department of Physics, Sejong University, Seoul, South Korea

[22] Department of Physics, University of Oslo, Oslo, Norway

[23] Dipartimento di Elettrotecnica ed Elettronica del Politecnico, Bari, Italy

[24] Dipartimento di Fisica dell'Università 'La Sapienza' and Sezione INFN Rome, Italy

[25] Dipartimento di Fisica dell'Università and Sezione INFN, Cagliari, Italy

[26] Dipartimento di Fisica dell'Università and Sezione INFN, Trieste, Italy

[27] Dipartimento di Fisica dell'Università and Sezione INFN, Turin, Italy

[28] Dipartimento di Fisica e Astronomia dell'Università and Sezione INFN, Bologna, Italy

[29] Dipartimento di Fisica e Astronomia dell'Università and Sezione INFN, Catania, Italy

[30] Dipartimento di Fisica e Astronomia dell'Università and Sezione INFN, Padova, Italy

[31] Dipartimento di Fisica 'E.R. Caianiello' dell'Università and Gruppo Collegato INFN, Salerno, Italy

[32] Dipartimento di Scienze e Innovazione Tecnologica dell'Università del Piemonte Orientale and Gruppo Collegato INFN, Alessandria, Italy

[33] Dipartimento Interateneo di Fisica 'M. Merlin' and Sezione INFN, Bari, Italy

[34] Division of Experimental High Energy Physics, University of Lund, Lund, Sweden

[35] Eberhard Karls Universität Tübingen, Tübingen, Germany

[36] European Organization for Nuclear Research (CERN), Geneva, Switzerland

[37] Excellence Cluster Universe, Technische Universität München, Munich, Germany

[38] Faculty of Engineering, Bergen University College, Bergen, Norway

[39] Faculty of Mathematics, Physics and Informatics, Comenius University, Bratislava, Slovakia

[40] Faculty of Nuclear Sciences and Physical Engineering, Czech Technical University in Prague, Prague, Czech Republic

[41] Faculty of Science, P.J. Šafárik University, Košice, Slovakia

[42] Faculty of Technology, Buskerud and Vestfold University College, Vestfold, Norway

[43] Frankfurt Institute for Advanced Studies, Johann Wolfgang Goethe-Universität Frankfurt, Frankfurt, Germany

[44] Gangneung-Wonju National University, Gangneung, South Korea

[45] Gauhati University, Department of Physics, Guwahati, India

[46] Helsinki Institute of Physics (HIP), Helsinki, Finland

[47] Hiroshima University, Hiroshima, Japan

[48] Indian Institute of Technology Bombay (IIT), Mumbai, India

[49] Indian Institute of Technology Indore, Indore (IITI), India

[50] Inha University, Incheon, South Korea

[51] Institut de Physique Nucléaire d'Orsay (IPNO), Université Paris-Sud, CNRS-IN2P3, Orsay, France

[52] Institut für Informatik, Johann Wolfgang Goethe-Universität Frankfurt, Frankfurt, Germany

[53] Institut für Kernphysik, Johann Wolfgang Goethe-Universität Frankfurt, Frankfurt, Germany

[54] Institut für Kernphysik, Westfälische Wilhelms-Universität Münster, Münster, Germany

[55] Institut Pluridisciplinaire Hubert Curien (IPHC), Université de Strasbourg, CNRS-IN2P3, Strasbourg, France

[56] Institute for Nuclear Research, Academy of Sciences, Moscow, Russia

[57] Institute for Subatomic Physics of Utrecht University, Utrecht, Netherlands

[58] Institute for Theoretical and Experimental Physics, Moscow, Russia

[59] Institute of Experimental Physics, Slovak Academy of Sciences, Košice, Slovakia

[60] Institute of Physics, Academy of Sciences of the Czech Republic, Prague, Czech Republic

[61] Institute of Physics, Bhubaneswar, India

[62] Institute of Space Science (ISS), Bucharest, Romania

[63] Instituto de Ciencias Nucleares, Universidad Nacional Autónoma de México, Mexico City, Mexico

[64] Instituto de Física, Universidad Nacional Autónoma de México, Mexico City, Mexico

[65] iThemba LABS, National Research Foundation, Somerset West, South Africa
[66] Joint Institute for Nuclear Research (JINR), Dubna, Russia
[67] Konkuk University, Seoul, South Korea
[68] Korea Institute of Science and Technology Information, Daejeon, South Korea
[69] KTO Karatay University, Konya, Turkey
[70] Laboratoire de Physique Corpusculaire (LPC), Clermont Université, Université Blaise Pascal, CNRS–IN2P3, Clermont-Ferrand, France
[71] Laboratoire de Physique Subatomique et de Cosmologie, Université Grenoble-Alpes, CNRS-IN2P3, Grenoble, France
[72] Laboratori Nazionali di Frascati, INFN, Frascati, Italy
[73] Laboratori Nazionali di Legnaro, INFN, Legnaro, Italy
[74] Lawrence Berkeley National Laboratory, Berkeley, California, United States
[75] Lawrence Livermore National Laboratory, Livermore, California, United States
[76] Moscow Engineering Physics Institute, Moscow, Russia
[77] National Centre for Nuclear Studies, Warsaw, Poland
[78] National Institute for Physics and Nuclear Engineering, Bucharest, Romania
[79] National Institute of Science Education and Research, Bhubaneswar, India
[80] Niels Bohr Institute, University of Copenhagen, Copenhagen, Denmark
[81] Nikhef, National Institute for Subatomic Physics, Amsterdam, Netherlands
[82] Nuclear Physics Group, STFC Daresbury Laboratory, Daresbury, United Kingdom
[83] Nuclear Physics Institute, Academy of Sciences of the Czech Republic, Řež u Prahy, Czech Republic
[84] Oak Ridge National Laboratory, Oak Ridge, Tennessee, United States
[85] Petersburg Nuclear Physics Institute, Gatchina, Russia
[86] Physics Department, Creighton University, Omaha, Nebraska, United States
[87] Physics Department, Panjab University, Chandigarh, India
[88] Physics Department, University of Athens, Athens, Greece
[89] Physics Department, University of Cape Town, Cape Town, South Africa
[90] Physics Department, University of Jammu, Jammu, India
[91] Physics Department, University of Rajasthan, Jaipur, India
[92] Physik Department, Technische Universität München, Munich, Germany
[93] Physikalisches Institut, Ruprecht-Karls-Universität Heidelberg, Heidelberg, Germany
[94] Politecnico di Torino, Turin, Italy
[95] Purdue University, West Lafayette, Indiana, United States
[96] Pusan National University, Pusan, South Korea
[97] Research Division and ExtreMe Matter Institute EMMI, GSI Helmholtzzentrum für Schwerionenforschung, Darmstadt, Germany
[98] Rudjer Bošković Institute, Zagreb, Croatia
[99] Russian Federal Nuclear Center (VNIIEF), Sarov, Russia
[100] Russian Research Centre Kurchatov Institute, Moscow, Russia
[101] Saha Institute of Nuclear Physics, Kolkata, India
[102] School of Physics and Astronomy, University of Birmingham, Birmingham, United Kingdom
[103] Sección Física, Departamento de Ciencias, Pontificia Universidad Católica del Perú, Lima, Peru
[104] Sezione INFN, Bari, Italy
[105] Sezione INFN, Bologna, Italy
[106] Sezione INFN, Cagliari, Italy
[107] Sezione INFN, Catania, Italy
[108] Sezione INFN, Padova, Italy
[109] Sezione INFN, Rome, Italy
[110] Sezione INFN, Trieste, Italy
[111] Sezione INFN, Turin, Italy
[112] SSC IHEP of NRC Kurchatov institute, Protvino, Russia
[113] SUBATECH, Ecole des Mines de Nantes, Université de Nantes, CNRS-IN2P3, Nantes, France
[114] Suranaree University of Technology, Nakhon Ratchasima, Thailand
[115] Technical University of Košice, Košice, Slovakia
[116] Technical University of Split FESB, Split, Croatia
[117] The Henryk Niewodniczanski Institute of Nuclear Physics, Polish Academy of Sciences, Cracow, Poland

[118] The University of Texas at Austin, Physics Department, Austin, Texas, USA
[119] Universidad Autónoma de Sinaloa, Culiacán, Mexico
[120] Universidade de São Paulo (USP), São Paulo, Brazil
[121] Universidade Estadual de Campinas (UNICAMP), Campinas, Brazil
[122] University of Houston, Houston, Texas, United States
[123] University of Jyväskylä, Jyväskylä, Finland
[124] University of Liverpool, Liverpool, United Kingdom
[125] University of Tennessee, Knoxville, Tennessee, United States
[126] University of the Witwatersrand, Johannesburg, South Africa
[127] University of Tokyo, Tokyo, Japan
[128] University of Tsukuba, Tsukuba, Japan
[129] University of Zagreb, Zagreb, Croatia
[130] Université de Lyon, Université Lyon 1, CNRS/IN2P3, IPN-Lyon, Villeurbanne, France
[131] V. Fock Institute for Physics, St. Petersburg State University, St. Petersburg, Russia
[132] Variable Energy Cyclotron Centre, Kolkata, India
[133] Vinča Institute of Nuclear Sciences, Belgrade, Serbia
[134] Warsaw University of Technology, Warsaw, Poland
[135] Wayne State University, Detroit, Michigan, United States
[136] Wigner Research Centre for Physics, Hungarian Academy of Sciences, Budapest, Hungary
[137] Yale University, New Haven, Connecticut, United States
[138] Yonsei University, Seoul, South Korea
[139] Zentrum für Technologietransfer und Telekommunikation (ZTT), Fachhochschule Worms, Worms, Germany